Available online at www.sciencedirect.com
SCIENCE DIRECT
Journal of Molecular Catalysis A: Chemical 247 (2006) 268–274
JOURNAL OF MOLECULAR CATALYSIS A: CHEMICAL
www.elsevier.com/locate/molcata

Sonochemical synthesis and visible light photocatalytic behavior of CdSe and CdSe/TiO_2 nanoparticles

Wingkei Ho, Jimmy C. Yu *

Department of Chemistry, The Chinese University of Hong Kong, Shatin, New Territories, Hong Kong, China

Received 6 October 2005; received in revised form 28 November 2005; accepted 29 November 2005
Available online 10 January 2006

Abstract

This paper reports an ultrasound-driven approach in the synthesis of CdSe and CdSe sensitized TiO_2 and also the their photocataltyic behavior of these materials under visible light. The results show that the CdSe/TiO_2 coupled system has a much higher photocatalytic activity than that of pure TiO_2 and CdSe in the degradation of 4-chlorophenol under visible light irradiation. The CdSe nanoparticles which act as a photosensitizer not only extend the spectral response of TiO_2 to the visible region but also reduce the charge recombination. Blue shift in the absorption onset confirms the size quantization of the CdSe nanoparticles under sonochemical synthesis. The quantum size effect alters the conduction and valence bands of CdSe particles to the appropriate energy levels in the coupled semiconductor system. This can make the electron injection from CdSe to TiO_2 more efficient and increase the degree of charge separation significantly, thereby enhancing the performance of the new coupled photocatalyst system.

Keywords: Titanium dioxide; Cadmium selenide, Sonochemical, Photocatalytic

1. Introduction

Titanium dioxide is a promising material for photoelectrochemical solar energy conversion and photocatalytic hazardous waste treatment because of its superior photoreactivity, nontoxicity, long-term stability and low price [1–6]. By coupling a second semiconductor to TiO_2, the photocatalytic efficiency and functionality can be further improved. The photocatalytic action of a semiconductor system is based on the generation of electron–hole pairs. In order to achieve a high reaction rate, the recombination of the charge carriers must be kept low. Coupling two semiconductors can result in the vectorial transfer of photo-generated electrons and holes from one semiconductor to another. This gives rise to charge separation and a decrease in the pair recombination rate, i.e. an increase of their lifetime [7–16]. Consequently, the availability of the pairs from the photocatalyst increases and an improvement in the occurrence of redox processes can be expected. In the past, Serpone et al. [17–21] have studied the photocatalytic behavior of several coupled semiconductor systems. Kamat and Patrick [22] have also demonstrated the simultaneous migration of both electrons and holes in coupled semiconductor photocatalysts. They found that the increase in the lifetime of the photo-generated pairs, due to hole and electron transfers between the two coupled semiconductors, was invoked in many cases as the key factor for the improvement of the photoactivity.

Another important feature of the coupled semiconductor system is that the photoresponse of a large band gap semiconductor can be extended into the visible region by coupling it with a short band gap semiconductor [23–27]. Conventionally, anatase TiO_2 only absorbs wavelength in the near-UV region ($\lambda \leq 390$ nm), which is about 3% of the solar spectrum. Thus, solar energy cannot be utilized efficiently in real applications. Fortunately, coupling TiO_2 with a smaller band gap semiconductor seems to be a promising approach to overcome this inherent limitation. In a coupled semiconductor system, the small band gap semiconductor that absorbs visible light acts as a photosensitizer for the TiO_2. Through the transfer of a photoexcited electron from the small band gap semiconductor to the TiO_2 particle, a photocatalytic redox reaction can occur. Thus, this photosensitization property of a coupled semiconductor system provides an alternative approach in the design of efficient visible light photocatalysts.

* Corresponding author. Tel.: +852 2609 6268; fax: +852 2603 5057.
E-mail address: jimyu@cuhk.edu.hk (J.C. Yu).

1381-1169/$ – see front matter © 2005 Elsevier B.V. All rights reserved.
doi:10.1016/j.molcata.2005.11.057

In an earlier study, we fabricated CdS-sensitized TiO_2 photocatalysts by a microemulsion-mediated solvothermal method [28]. It was shown that the excitation of CdS which had been coupled with TiO_2 resulted in electron injection into the lower-lying conduction band of the TiO_2. The effectiveness of this new photocatalyst was demonstrated by the decomposition of methylene blue under visible light irradiation. In addition, we have also revealed that nanoclusters of MoS_2 and WS_2 can be coupled to TiO_2 by an in situ photo-reduction deposition method which takes advantage of the reducing power of the photo-generated electrons from TiO_2 particles [29]. The coupling of TiO_2 photocatalyst with quantum-sized MoS_2 and WS_2 nanoclusters exhibited visible light activity in the degradation of methylene blue and 4-chlorophenol.

Here, we report for the first time on the coupling of TiO_2 with a small band gap semiconductor (CdSe) by an ultrasound-driven synthesis approach. CdSe is chosen as the photosensitizer for TiO_2 in our study because its energy gap $E_g = 1.7$ eV which closely matches the solar spectrum [30,31]. Moreover, it is important to note that the conduction band minimum of the small band gap semiconductor should be higher than that of TiO_2 so that the transfer of the photo-generated electron is allowed from the former to the latter one. The conduction band energy level (ECB) of CdSe is about −1.0 V versus NHE, which is more negative than that of TiO_2 (ECB about −0.5 V versus NHE). This entirely fulfills the required condition in the CdSe/TiO_2 coupled semiconductor system [32]. In addition, CdSe exhibits much greater photostability than organic dyes when used as a photosensitizer. Therefore, many attempts have been made to use CdSe to photosensitize TiO_2 in visible light. Rincon et al. [33,34] have reported the photovoltaic conversion of TiO_2 coatings sensitized with chemically deposited CdSe thin films. Fang et al. [35,36] have also showed that modification of the TiO_2 electrode with CdSe particles could extend the optical absorption spectrum and photocurrent action spectrum into the visible range. However, there is no report on the utilization of CdSe/TiO_2 photocatalyst systems for environmental purification under visible light irradiation.

Sonochemical processing has been proven to be a useful technique for generating novel materials with unusual properties [37–44]. The powerful ability of ultrasound to affect chemical changes arises from cavitation phenomenon involving the formation, growth and collapse of bubbles in liquid. The implosive collapse of bubbles generates localized hot spots through adiabatic compression within the gas phase of the collapsing bubble. The conditions formed in these hot spots have been experimentally determined, with transient temperatures of about 5000 K, pressures of 1800 atm and cooling rates in excess of 108 K/s. The energy provided by the ultrasound radiation is high enough to enable many chemical reactions to occur. Compared to the conventional CdSe/TiO_2 synthesis [33–36], which requires thermal treatment at 673–723 K to induce and improve the crystallinity of the chemically deposited CdSe layer, sonochemical preparation is more effective as it takes advantage of the ultrasonic power for the crystallization of CdSe. The crystalline CdSe can be dispersively formed and inherently bound on TiO_2 particles without any post-thermal treatment.

In this paper, we describe a detailed study of using sonochemical synthesized CdSe to photosensitize TiO_2 particles for the photocatalytic purification. The experimental results reveal that the sensitization of TiO_2 with CdSe not only extended the optical absorption spectrum into visible range, but also exhibits visible light activity in the degradation of 4-chlorophenol. In addition, the optical properties of the sonochemical synthesized CdSe and CdSe/TiO_2 correlated with the size quantization will also be discussed. The purpose of this work is to elucidate the importance of coupled semiconductor systems (CdSe/TiO_2) in comparison to single semiconductor systems (CdSe) on visible light photocatalysis.

2. Experimental section

2.1. Sonochemcial preparation of CdSe sensitized TiO_2

All chemicals used in this study were reagent grade supplied from Aldrich and were used as received.

In a 250 ml conical flask, Na_2SeO_3 (0.0025 mol) was first added into the $N_2H_4{\cdot}H_2O$ solution (5 ml). A mixture of $Cd(NO_3)_2$ (0.005 mol) and $NH_3{\cdot}H_2O$ (3 ml) was then added to the above solution under ultrasound irradiation produced by a commercial ultrasonic cleaning bath (Branson, USA, model 3210E, DTH, 47 kHz, 120 W). After 2 h sonication, an orange precipitate (amorphous CdSe) was obtained. Then, different amounts of the TiO_2 (Degussa P25) powder were added into the solution mixture, followed by further sonication for the crystallization of CdSe. The resulting powders (a precipitate of crimson material) were recovered by filtration, then washed with a 0.1 M acetic acid aqueous solution and ethanol thoroughly, and finally dried in an oven at 100 °C. During the sonication, the temperature of water in the ultrasonic cleaning bath was about 50 °C. For comparison, identical control experiments were performed without using ultrasound irradiation.

2.2. Characterization

X-ray photoelectron spectroscopy (XPS) measurements were performed on a PHI Quantum 2000 XPS System with a monochromatic Al Kα source and a charge neutralizer. All the binding energies were referenced to the C 1s peak at 284.8 eV of the surface adventitious carbon. The X-ray diffraction (XRD) patterns, obtained on a Bruker D8 Advance X-ray diffractometer using Cu Kα radiation at a scan rate of $0.05^\circ\ 2\theta\,s^{-1}$, were used to identify the phase constitutions in samples and their crystallite size. The accelerating voltage and the applied current were 40 kV and 40 mA, respectively. The crystallite size was calculated from X-ray line broadening analysis by Scherrer formula. UV–vis diffuse reflectance spectra were achieved using a UV–vis spectrophotometer (Cary 100 Scan Spectrophotometers, Varian, USA). High-resolution transmission electron microscopy (HRTEM) images were taken by a JEOL 2010 TEM operated at a 200 kV accelerating voltage with energy-dispersive X-ray analysis (EDX). The EPR spectrum was recorded on an X-band EPR spectrom-

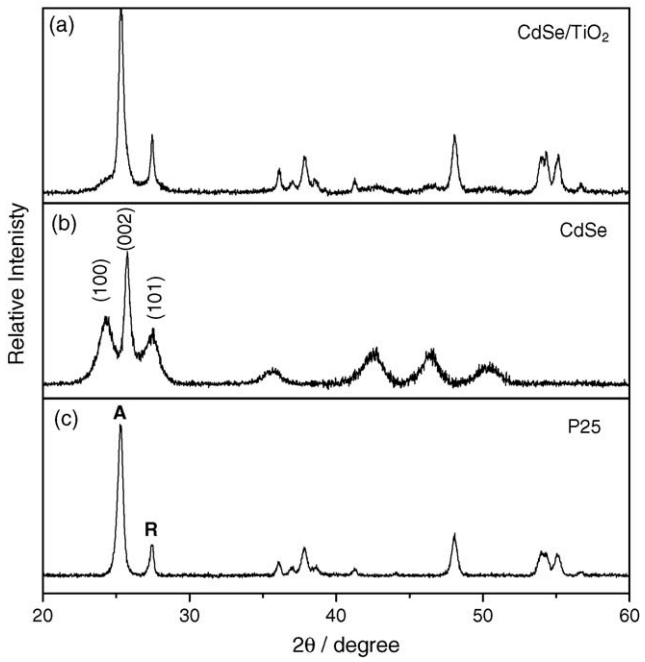

Fig. 1. XRD patterns of (a) $CdSe/TiO_2$, (b) pure CdSe, and (c) TiO_2 (P25). "A" and "R" represent the peaks of anatase and rutile phases, respectively.

eter (JEOL, JES-TE100) at 77 K. The sample was irradiated by a 500 W super high-pressure mercury lamp (Ushio, USH500D) equipped with a bandpass filter of 424 nm (Toshiba, Y-44).

2.3. Photocatalytic activity measurements

The photocatalytic activities of the CdSe sensitized TiO_2 samples were measured by the degradation of 4-chlorophenol in an aqueous solution. O_2 was bubbled into the solution throughout the experiment. A 300 W tungsten halogen lamp with a 400 nm cut off filter was used as visible light source. 0.2 g of photocatalyst was suspended in a 200 ml aqueous solution of 2.5×10^{-4} M 4-chlorophenol. The concentrations of 4-chlorophenol and its degradation products were measured with a HPLC system (Waters Baseline 810) with a Waters 486 tunable UV absorbance detector. A Supelco LC-18-DB column (250 mm × 4.6 mm) was applied. The eluent consisted of a 40:60 methanol:water mixture, and the flow rate was 1 ml/min. The aromatic compounds were detected at 220 nm. Millipore discs were used to separate the catalysts before analysis of the solution.

Total organic carbon (TOC) was also measured in the 4-chlorophenol degradation processes using a TOC analyzer (Shimadzu, TOC 5000). 0.2 g of photocatalyst was suspended in a 100 ml aqueous solution of 2.5×10^{-4} M 4-chlorophenol. The TOC analysis was carried out after removal of catalyst particles by filtration with Millipore filter.

3. Results and discussion

Fig. 1 shows the XRD patterns of the pure TiO_2 (P25), and the sonochemically synthesized CdSe and $CdSe/TiO_2$. The characteristic peaks corresponding to (1 0 0), (0 0 2) and (1 0 1)

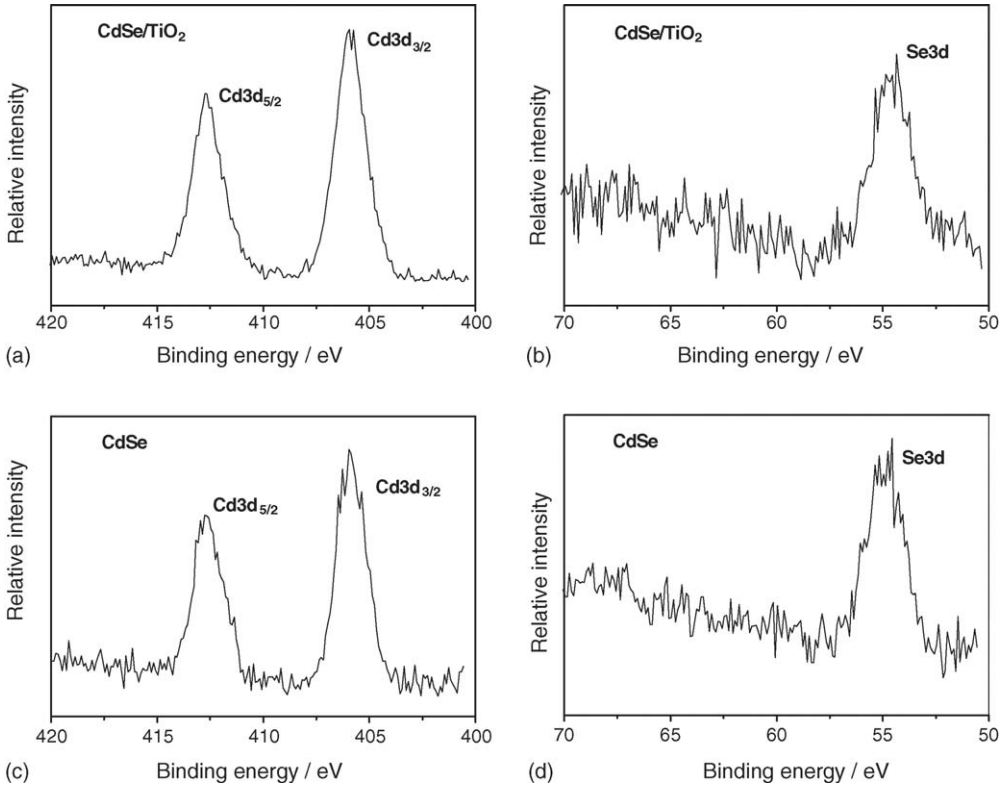

Fig. 2. High-resolution XPS spectra of the Cd 3d and Se 3d regions for the (a and b) $CdSe/TiO_2$ and (c and d) pure CdSe.

crystal planes of CdSe were detected from the sonochemically synthesized CdSe (Fig. 1b). These peaks can be indexed to a pure hexagonal CdSe wurtzite structure (JCPDS, no. 77-2307) with an average crystallite size of 9.5 nm as determined by the Debye–Scherrer equation [45]. The diffractogram of the sonochemical synthesized CdSe/TiO_2 (Fig. 1c) suggests the presence of anatase and rutile crystals as well as a small amount of CdSe hexagonal structure. It should be note that no CdSe peaks were observed when the experiment was carried out without ultrasound irradiation. This indicates that the ultrasonic irradiation is responsible for the formation of the CdSe/TiO_2 composite.

The elemental compositions of the sonochemically synthesized CdSe and CdSe/TiO_2 were analyzed by XPS. In the high-resolution XPS spectra (Fig. 2a and b), the Cd $3d_{3/2}$ at 405.3 eV and Cd $3d_{5/2}$ at 411.8 eV as well as Se 3d at 53.4 eV in the sonochemically synthesized CdSe sample confirms the existence of Cd^{2+} and Se^{2-} ions, respectively [46,47]. Similarly, the two adjacent strong peaks at 405.2 and 411.8 eV corresponding to the binding energy of Cd 3d and peak at 53.6 eV corresponding to the binding energy of Se 3d were also observed from the CdSe/TiO_2 sample in Fig. 2c and d. In addition, the quantification of peaks gives the ratio of Cd to Se as about 1:1 for both samples. No obvious peaks for cadmium oxide, hydroxide and selenium oxide were detected in the samples indicating the high purity of CdSe in the sonochemically synthesized products.

Transition electron microscopy with energy-dispersive X-ray spectroscopy provides information on the morphology, crystallinity and chemical composition of the coupled semiconductor photocatalysts. Fig. 3a shows the TEM image of CdSe/TiO_2 particles which are spherical in shape and with an average size of about 60 nm. Chemical composition analysis of the coupled semiconductor was examined by energy-dispersive X-ray spectroscopy. Signals corresponding to Cd and Se were detected in all the regions selected in the CdSe/TiO_2 sample (Fig. 4). The EDX results reveal the presence of CdSe with a higher content at zones D, E & F and lower content of CdSe at zone G. This suggests that the "darker" particles appearing in the micrograph are an indicative of denser agglomeration of CdSe on TiO_2 particles. In a high-resolution TEM image of zone E (Fig. 3b), well-resolved lattice fringes were found. The clear fringes on the micrograph allow an accurate measurement of crystallographic spacing and identification of the observed crystallites. The lattice spacing measured from the fringes (3.7 Å) in Fig. 3b is consistent with the bulk value of hexagonal CdSe ($d_{(1\,0\,0)}$ = 3.72 Å). Noticeably, the above results agree with those of high-resolution X-ray photoelectron spectroscopy in which Cd^{2+} and Se^{2-} were detected in the CdSe/TiO_2. This indicates that the CdSe was successfully synthesized and deposited on TiO_2 particles after the sonochemical process.

Fig. 5 shows the UV–vis diffuse reflectance spectra of the pure TiO_2, CdSe and CdSe/TiO_2. The bare TiO_2 exhibits the fundamental absorption edge corresponding to the band gap energy of 3.2 eV in the ultraviolet region. The absorption onset of the sonochemically synthesized CdSe is found at around 580 nm and its band gap (E_g) was calculated to be 2.1 eV. Compared

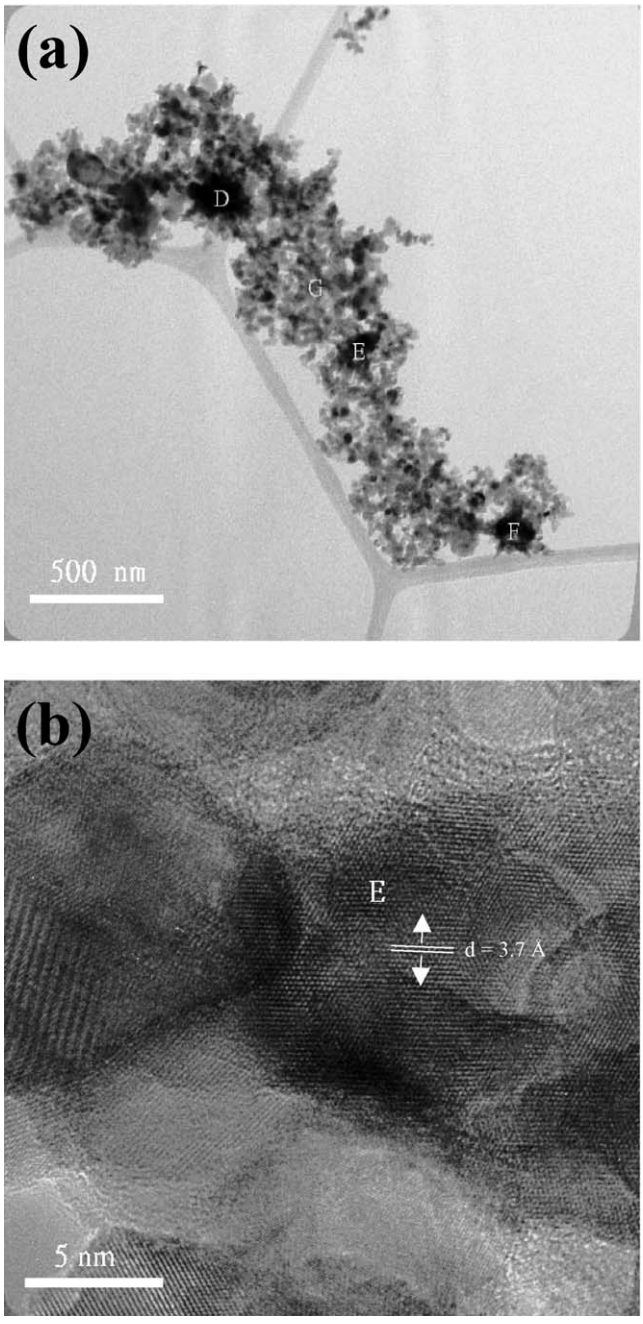

Fig. 3. (a) TEM images of sonochemically synthesized CdSe/TiO_2. Regions (D–G) were selected for EDX microanalysis. (b) HRTEM micrographs at 200 kV of region E in (a) for the CdSe/TiO_2 sample.

with that of bulk crystalline CdSe, which has the absorption onset at about 710 nm (E_g = 1.74 eV) [48,49], nearly 130 nm of blue shift was observed for the synthesized CdSe. The blue shift in the absorbance indicates an increase in the band gap energy of CdSe. Since the absorption edge is an index of particle size, smaller CdSe particles formed in the sonochemical preparation led to the larger band gap and shorter wavelength in absorption. Thus, this shift clearly reflects the presence of quantum size effects in the pure CdSe under the sonochemical synthesis [50]. When the TiO_2 is coupled with the CdSe particles, it displays the characteristic absorption of CdSe in visible region in

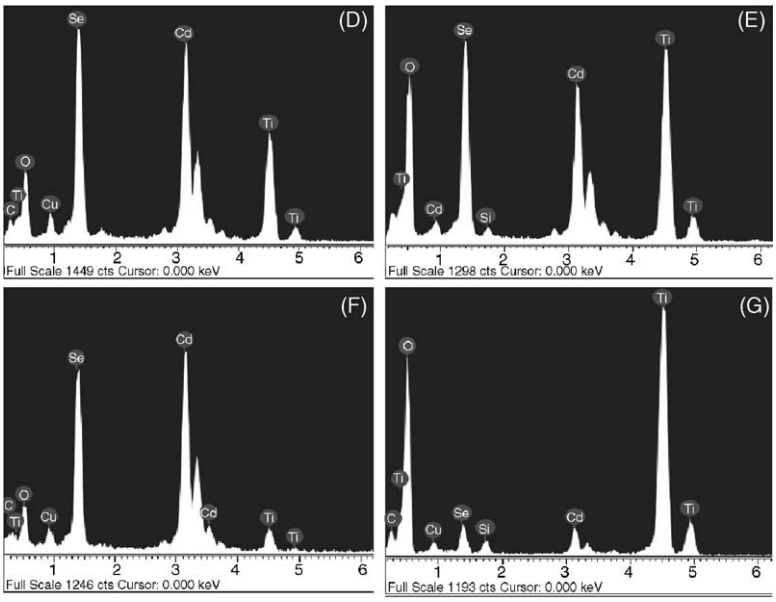

Fig. 4. EDX microanalysis spectra of the CdSe/TiO_2 (regions D, E, F & G). The X-ray excitation energy for Cd and Se are about 3.1 and 1.4 keV, respectively.

the spectrum. As the quantum-sized CdSe crystallites deposit on the TiO_2 particles during sonochemical process, the optical absorption of the CdSe/TiO_2 coupled system can be extended into the visible region.

4-Chlorophenol was selected as the target substrate in this study. Fig. 6 illustrates the photocatalytic degradation of 4-chlorophenol in the presence of CdSe/TiO_2 samples. The results indicate that CdSe sensitized TiO_2 was efficient in the photo-degradation of 4-chlorophenol under visible light irradiation. The concentration of 4-chlorophenol dropped to about 68% after 8 h irradiation. However, pure CdSe degraded the 4-chlorophenol gradually to about only 89%, which may due to its higher recombination rate of charges. No photo-degradation of 4-chlorophenol occurs when pure TiO_2 is irradiated with visible light, since it is inactive under visible light irradiation ($\lambda > 400$ nm).

To further verify whether 4-chlorophenol was mineralized, the total organic carbon (TOC) analysis was performed. TOC values reflect the amount of organics in the solution. Therefore, the changes in TOC mirror the degree of mineralization of an organic substrate during the irradiation period. Fig. 7 depicts the decays of TOC in the degradation of 4-chlorophenol for the samples. Upon visible light irradiation of the dispersions, nearly 22% reduction of TOC was observed in the coupled sample after 8 h irradiation. However, only a 10% decrease in TOC was found for the pure CdSe and no mineralization of 4-chlorophenol was observed for pure TiO_2.

The improvement of the photocatalytic performance can be attributed to the coupling semiconductor system. The advantages of using such coupled semiconductor systems are twofold: (i) to extend the photoresponse of large bandgap semiconductors; (ii)

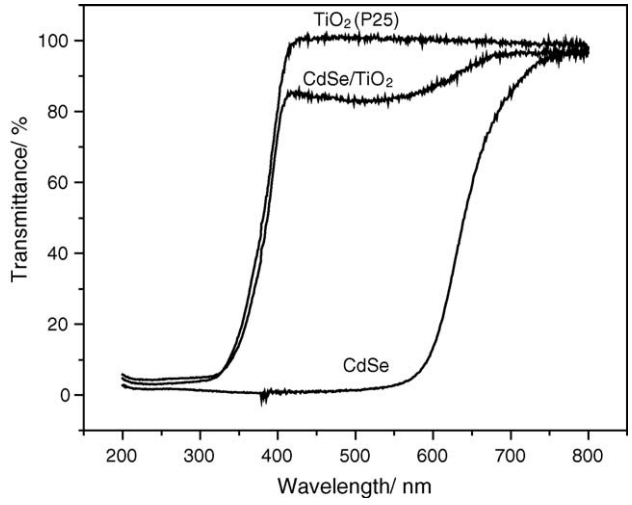

Fig. 5. UV–vis diffuse reflectance spectra of pure TiO_2, CdSe and CdSe/TiO_2.

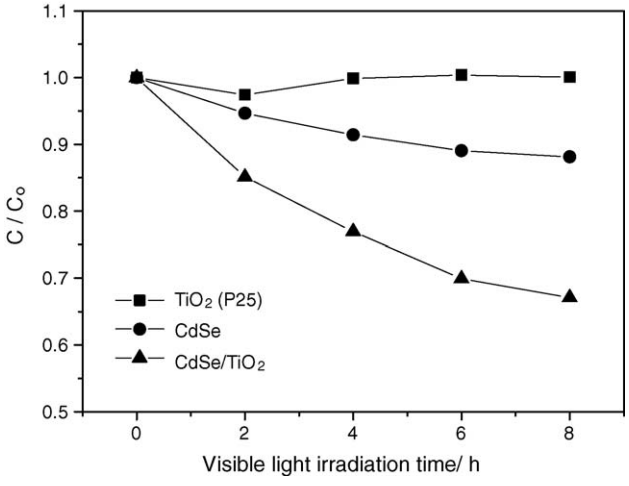

Fig. 6. Photo-degradation of 4-chlorophenol for the pure TiO_2, CdSe and CdSe sensitized TiO_2 under visible light irradiation ($\lambda > 400$ nm). *C* represents the concentration of 4-chlorophenol measured by HPLC.

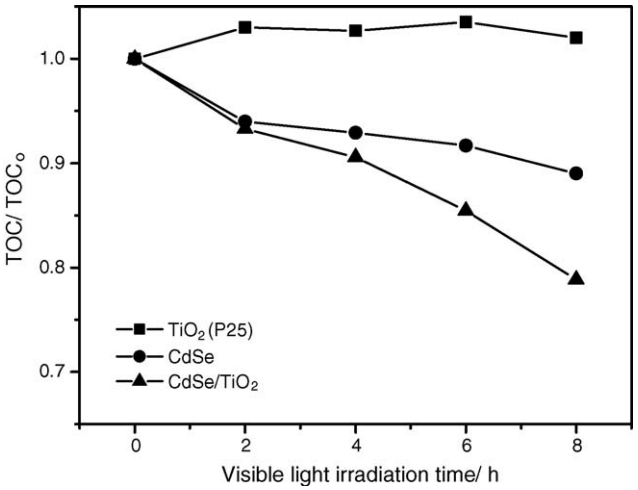

Fig. 7. TOC photo-degradation of 4-chlorophenol for the pure TiO_2, CdSe and CdSe sensitized TiO_2 under visible light irradiation ($\lambda > 400$ nm).

to retard the recombination of photo-generated charge carriers by injecting electrons into the lower-lying conduction band of large bandgap semiconductors such as TiO_2.

First, it is well known that pure TiO_2 does not exhibit visible light photocatalytic activity. However, the photoresponse of TiO_2 could be extended into the visible region after coupling with CdSe. The appropriate energy levels of the conduction and valence bands allow CdSe to act as sensitizers for visible light TiO_2 photocatalysis in the degradation of 4-chlorophenol.

Secondly, compared to that of pure CdSe, the visible light photocatalytic efficiency can be improved in the coupled system. The enhancement of the photocatalytic activity for the CdSe/TiO_2 system compared with that of pure CdSe can be ascribed to the effective charge carrier separation and transportation throughout the particles [51,52]. Under visible light irradiation, only CdSe can be activated. The conduction band level of CdSe is deemed to be higher than that of TiO_2. This may facilitate the interfacial electron transfer from CdSe to TiO_2. The photo-generated electrons are injected from the conduction band of CdSe into TiO_2 and accumulate at the lower-lying conduction band of TiO_2. A signal identified to Ti^{3+} radical ($g = 1.992$) is detected in the ESR spectrum (Fig. 8), which indicates the migration of photo-generated electrons from the

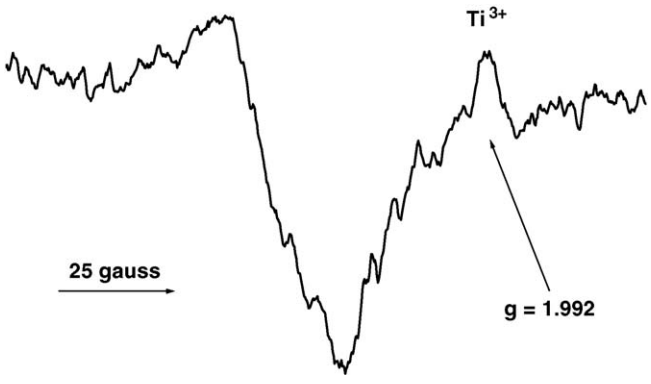

Fig. 8. ESR spectrum of CdSe sensitized TiO_2 powder recorded at 77 K in the presence of oxygen under visible light ($\lambda > 425$ nm) irradiation.

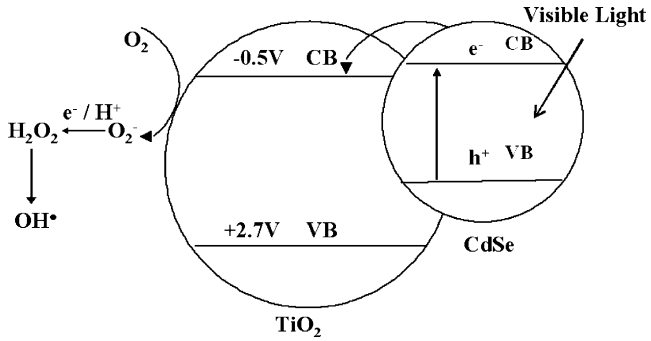

Fig. 9. Schematic diagram representing the inter-particle charge transfer process in a CdSe/TiO_2 coupled system.

conduction band of CdSe to that of TiO_2 under visible light [53,54]. Consequently, the photo-generated electron is scavenged by the oxygen in water, hence forming hydroxyl radicals to degrade the 4-chlorophenol (Fig. 9). Thus, in the presence of TiO_2 as the coupling partner, the e^- and h^+ pairs originally generated in a CdSe particle find themselves in different semiconductor particles shortly afterwards, i.e. an efficient charge separation is achieved.

In addition, the phenomenon of size quantization in the CdSe particles prepared by the sonochemical method also plays an important role for the enhancement of photocatalytic efficiency. The blue shifts in the absorption spectra for the CdSe and CdSe/TiO_2 samples clearly reveal the quantum size effect. When the band gap increases, both the conduction band and valence bands of the quantum-sized CdSe in the coupled samples become more cathodic and anodic, respectively. The conduction band level of CdSe shifts to a more negative value, which favors electron injection from the photoexcited CdSe into TiO_2. The electron injection to TiO_2 has to compete with the charge recombination in the CdSe particle. In order to make the electron injection fast enough, a certain driving force has to exist. This driving force for the electron transfer between CdSe and TiO_2 particles is the relative energy difference between the conduction bands of two semiconductors. The difference becomes greater with decreasing CdSe particle size. Thus, for quantized particles of CdSe, the bottom of the conduction band for CdSe becomes higher and the electron injection is more efficient. Undoubtedly, the size quantization of CdSe promotes the photocatalytic efficiency of the coupled semiconductor system and plays a dominant role in the significant increase of visible light photocatalytic activity.

4. Conclusion

This study demonstrates the fabrication of CdSe sensitized TiO_2 by using a sonochemical approach. The quantum-sized CdSe photosensitizer not only extends the spectral response of TiO_2 to the visible region but also allows interparticle electron transfer. The Ti^{3+} signal observed in ESR measurement confirms the displacement of electrons from CdSe to TiO_2. Such a binary photocatalyst system is worth exploring in designing novel solar energy conversion devices.

Acknowledgements

This work was supported by a grant from the Research Grants Council of the Hong Kong Special Administrative Region, China (Project No. CUHK4027/02P). We acknowledge Dr Daniel Kwong and Ms Anna Chan of Hong Kong Baptist University for their assistance in ESR measurements.

References

[1] M.S. Hoffmann, T. Martin, W. Choi, D.W. Bahnemann, Chem. Rev. 95 (1995) 69.
[2] M.A. Fox, M.T. Duby, Chem. Rev. 93 (1993) 341.
[3] P.V. Kamat, Chem. Rev. 93 (1993) 267.
[4] A.L. Linsebigler, G. Lu Jr., J.T. Yates, Chem. Rev. 95 (1995) 735.
[5] A. Fujishima, T.N. Rao, D.A. Tryk, J. Photochem. Photobiol. C: Photochem. Rev. 1 (2000) 1.
[6] D.F. Ollis, H. Al-Ekabi, Photocatalytic Purification and Treatment of Water and Air, Elsevier Sci. Pub., New York, 1993.
[7] Y.T. Kwon, K.Y. Song, W.I. Lee, G.J. Choi, Y.R. Do, J. Catal. 191 (2000) 192.
[8] Y. Cao, X. Zhang, W. Yang, H. Du, Y. Bai, T. Li, J. Yao, Chem. Mater. 12 (2000) 3445.
[9] H. Tada, A. Hattori, Y. Tokihisa, K. Imai, N. Tohge, S. Ito, J. Phys. Chem. B 104 (2000) 4585.
[10] K. Vinodgopal, I. Bedja, P.V. Kamat, Chem. Mater. 8 (1996) 2180.
[11] I. Bedja, P.V. Kamat, J. Phys. Chem. 99 (1995) 9182.
[12] K. Vinodgopal, P.V. Kamat, Environ. Sci. Technol. 29 (1995) 841.
[13] A. Hattori, Y. Tokihisa, H. Tada, N. Tohge, S. Ito, K. Hongo, R. Shiratsuchi, G. Nogami, J. Sol–Gel Sci. Technol. 22 (2001) 53.
[14] G. Marci, V. Augugliaro, M.J. Lopez-Munoz, C. Martin, L. Palmisano, V. Rives, M. Schiavello, R.J.D. Tilley, A.M. Venezia, J. Phys. Chem. B 105 (2001) 1026.
[15] G. Marci, V. Augugliaro, M.J. Lopez-Munoz, C. Martin, L. Palmisano, V. Rives, M. Schiavello, R.J.D. Tilley, A.M. Venezia, J. Phys. Chem. B 105 (2001) 1033.
[16] J. Bandara, C.C. Hadapangoda, W.G. Jayasekera, Appl. Catal. B: Environ. 50 (2004) 83.
[17] N. Serpone, P. Maruthamuthu, P. Pichat, E. Pelizzetti, H. Hidaka, J. Photochem. Photobiol. A: Chem. 85 (1995) 247.
[18] N. Serpone, E. Borgarello, M. Graetzel, J. Chem. Soc., Chem. Commun. (1984) 342.
[19] N. Serpone, E. Borgarello, E. Pelizzetti, M. Barbeni, Chim. Ind. (Milano) 67 (1985) 318.
[20] N. Serpone, E. Borgarello, E. Pelizzetti, J. Electrochem. Soc. 135 (1988) 2760.
[21] P. Pichat, E. Borgarello, J. Disdier, M. Hermann, E. Pelizzetti, N. Serpone, J. Chem. Soc., Faraday Trans. 1 (84) (1988) 261.
[22] P.V. Kamat, B. Patrick, J. Phys. Chem. 96 (1992) 6829.
[23] R. Vogel, K. Pohl, H. Weller, Chem. Phys. Lett. 174 (1990) 241.
[24] A.S. Suleymanov, Int. J. Hydrogen Energy 16 (1991) 741.
[25] A. Ennaoui, S. Fiechter, H. Tributsch, M. Giersig, R. Vogel, H. Weller, J. Electrochem. Soc. 139 (1992) 2514.
[26] S. Hotchandaui, P.V. Kamat, J. Phys. Chem. 96 (1992) 6834.
[27] S. Hotchandaui, P.V. Kamat, Chem. Phys. Lett. 91 (1992) 3204.
[28] J.C. Yu, L. Wu, J. Lin, P. Li, Q. Li, Chem. Commun. (2003) 1552.
[29] W. Ho, J.C. Yu, J. Lin, J. Yu, P. Li, Langmuir 20 (2004) 5865.
[30] J.J. Zhu, O. Palchik, S. Chen, A. Gedanken, J. Phys. Chem. B 104 (2000) 7344.
[31] J.O. Joswig, S. Roy, P. Sarkar, M. Springborg, Chem. Phys. Lett. 365 (2002) 75.
[32] D. Liu, P.V. Kamat, J. Phys. Chem. 97 (1993) 10769.
[33] M.E. Rincon, A. Jimenez, A. Orihuela, G. Martinez, Sol. Energy Mater. Sol. Cells 52 (1998) 399.
[34] M.E. Rincon, O. Gomez-Daza, C. Corripio, A. Orihuela, Thin Solid Films 389 (2001) 91.
[35] J.H. Fang, X.M. Lu, X.F. Zhang, D.G. Fu, Z.H. Lu, Supramol. Sci. 5 (1998) 709.
[36] J.H. Fang, J.W. Wu, X.M. Lu, Y.C. Shen, Z.H. Lu, Chem. Phys. Lett. 270 (1997) 145.
[37] K.S. Suslick, S.B. Choe, A.A. Cichowals, M.W. Grinstaff, Nature 353 (1991) 414.
[38] K.S. Suslick, G.J. Price, Annu. Rev. Mater. Sci. 29 (1999) 295.
[39] A. Gedanken, X. Tang, Y. Wang, N. Perkas, Y. Koltypin, M.V. Landau, L. Vradman, M. Herskowitz, Chem. Eur. J. 7 (2001) 4546.
[40] J. Zhu, Y. Koltypin, A. Gedanken, Chem. Mater. 12 (2000) 73.
[41] V.G. Pol, R. Reisfeld, A. Gedanken, Chem. Mater. 14 (2002) 3920.
[42] N.A. Dhas, A. Zaban, A. Gedanken, Chem. Mater. 11 (1999) 806.
[43] V.G. Pol, M. Motiei, A. Gedanken, J. Calderon-Moreno, Y. Mastai, Chem. Mater. 15 (2003) 1378.
[44] N.A. Dhas, A. Gedanken, Appl. Phys. Lett. 72 (1998) 2514.
[45] J.P. Ge, Y.D. Li, G.Q. Yang, Chem. Commun. (2002) 1826.
[46] C. Wagner, G. Muilnberg, Handbook of X-ray Photoelectron Spectroscopy, Physical Electronics Division, Perkin-Elmer Corporation, Eden Prairie, MN, 1979.
[47] E. Hao, H. Sun, Z. Zhou, J. Liu, B. Yang, J. Shen, Chem. Mater. 11 (1999) 3096.
[48] Y. Mastai, R. Polsky, Y. Koltypin, A. Gedanken, G. Hodes, J. Am. Chem. Soc. 121 (1999) 10047.
[49] G. Kortum, Reflectance Spectroscopy, Springer, Berlin, 1973.
[50] C.B. Murry, J. Norris, M.G. Bawendi, J. Am. Chem. Soc. 115 (1993) 8706.
[51] L. Spanhel, H. Weller, A. Henglein, J. Am. Chem. Soc. 109 (1987) 6632.
[52] P.A. Sant, P.V. Kamat, Phys. Chem. Chem. Phys. 4 (2002) 198.
[53] R.F. Howe, M. Gratzel, J. Phys. Chem. 91 (1987) 3906.
[54] M. Gratzel, R.F. Howe, J. Phys. Chem. 94 (1990) 2566.